

QCD sum rule analysis of the decays $B \rightarrow K \ell^+ \ell^-$ and $B \rightarrow K^* \ell^+ \ell^-$

P. Colangelo,¹ F. De Fazio,^{1,2} P. Santorelli,³ and E. Scrimieri^{1,2}

¹*Istituto Nazionale di Fisica Nucleare, Sezione di Bari, Italy*

²*Dipartimento di Fisica dell'Università di Bari, via G. Amendola 173, 70126 Bari, Italy*

³*Dipartimento di Fisica dell'Università "Federico II" di Napoli and Istituto Nazionale di Fisica Nucleare, Sezione di Napoli, Mostra D'Oltremare, Pad 19-20, 80125 Napoli, Italy*

(Received 25 October 1995)

We use QCD sum rules to calculate the hadronic matrix elements governing the rare decays $B \rightarrow K \ell^+ \ell^-$ and $B \rightarrow K^* \ell^+ \ell^-$ induced by the flavor-changing neutral current $b \rightarrow s$ transition. We also study relations among semileptonic and rare $B \rightarrow K^{(*)}$ decay form factors. The analysis of the invariant mass distribution of the lepton pair in $B \rightarrow K^{(*)} \ell^+ \ell^-$ and of the angular asymmetry in $B \rightarrow K^* \ell^+ \ell^-$ provides us with interesting tests of the standard model and its extensions.

PACS number(s): 13.20.He, 11.55.Hx, 12.38.Cy

I. INTRODUCTION

Rare B -meson decays induced by the flavor-changing neutral current $b \rightarrow s$ transition represent important channels for testing the standard model (SM) and for searching for the effects of possible new interactions [1]. As a matter of fact, these processes, which in SM do not occur in the Born approximation, are particularly sensitive to perturbative QCD corrections and to possible higher mass scales and interactions predicted in supersymmetric theories, two Higgs doublet, and top-color, left-right models, etc. Such interactions determine the operators and their Wilson coefficients appearing in the low energy $\Delta B = 1$ effective Hamiltonian H_W that governs the $b \rightarrow s$ transition.

From the experimental point of view, the radiative $b \rightarrow s \gamma$ decay has been observed and measured by the CLEO II Collaboration both in the inclusive $B \rightarrow X_s \gamma$ and exclusive $B \rightarrow K^* \gamma$ modes; the experimental results

$$B(b \rightarrow s \gamma) = (2.32 \pm 0.57 \pm 0.35) \times 10^{-4} \quad [2] \quad (1.1)$$

and

$$B(\bar{B}^0 \rightarrow K^{*0} \gamma) = (4.0 \pm 1.7 \pm 0.8) \times 10^{-5} \quad [3], \quad (1.2)$$

$$B(B^- \rightarrow K^{*-} \gamma) = (5.7 \pm 3.1 \pm 1.1) \times 10^{-5} \quad [3],$$

have prompted a number of analyses aimed at restricting the parameter space of various extensions of the standard model [4]. Similar analyses have also been proposed for the transition $b \rightarrow s \ell^+ \ell^-$, which has not been observed yet [5]; in this case, the invariant dilepton mass distribution and the asymmetry of the dilepton angular distribution, together with the total decay rate, can be used to study the features of the interaction inducing the decay. However, for the exclusive modes such as $B \rightarrow K \ell^+ \ell^-$ and $B \rightarrow K^* \ell^+ \ell^-$ one has to face the problem of computing the matrix element of H_W between the states B and K , K^* , a problem related to the nonperturbative sector of QCD.

For these matrix elements, either specific hadronization models [6,7] or information from two-point function QCD sum rules [8] and from the heavy meson chiral theory [9], embedded in the vector meson dominance framework, have

been used so far. The resulting theoretical predictions are characterized by a considerable model dependence; it should be noticed that, differently from the case of $B \rightarrow K^* \gamma$, where the hadronic matrix element must be computed only at one kinematical point, in correspondence to the on-shell photon, for $B \rightarrow K \ell^+ \ell^-$ and $B \rightarrow K^* \ell^+ \ell^-$ the matrix elements must be known in a wide range of the invariant mass squared of the lepton pair: $M_{\ell^+ \ell^-}^2 = [4M_\ell^2, (M_B - M_{K,K^*})^2]$; therefore, the vector meson dominance assumption has non-negligible consequences on the theoretical outcome.

An approach based on general features of QCD that allows us to compute the hadronic matrix elements in a range of $M_{\ell^+ \ell^-}^2$ is provided by three-point function QCD sum rules [10]. This method, first employed to compute the pion form factor [11], has been widely applied to heavy meson semileptonic decays: For example, in the case of $B \rightarrow D, D^*$ semileptonic transitions, it has been used to compute the Isgur-Wise universal function $\xi(y)$ and the heavy quark mass corrections [12]. Moreover, the decays $B \rightarrow D^{**} \ell \nu$, where D^{**} are positive parity ($c\bar{q}$) meson states, have been analyzed both for finite heavy quark masses [13] and in the limit $m_Q \rightarrow \infty$, with the calculation of the universal functions $\tau_{1/2}(y)$ and $\tau_{3/2}(y)$ analogous to the Isgur-Wise function [14]. For the heavy-to-light meson transitions, such as $D(B) \rightarrow \pi(\rho) \ell \nu$, the various matrix elements have also been computed [15,16]; in the case of $B \rightarrow K^* \gamma$, this approach, employed in [17–19], has provided us with the prediction $R = B(B \rightarrow K^* \gamma) / B(b \rightarrow s \gamma) = 0.17 \pm 0.05$ [17], which agrees with the central value obtained from the experimental data in Eqs. (1.1) and (1.2).

In this paper we want to apply the three-point function QCD sum rule method to compute the hadronic quantities appearing in the calculation of $B \rightarrow K^{(*)} \ell^+ \ell^-$. We shall observe that the various form factors parametrizing the relevant matrix elements have common features with other heavy-to-light meson transitions, a behavior whose origin is worth investigating in detail [20]. We shall also compare the computed hadronic quantities to the findings of lattice QCD, even though these last results are obtained after extrapolations in the heavy quark mass and in the momentum transfer. Finally, we shall apply our results to predict the invariant mass distribution of the lepton pair in the decays

$B \rightarrow K^{(*)} \ell^+ \ell^-$ and the forward-backward asymmetry for $B \rightarrow K^* \ell^+ \ell^-$ in the standard model.

The work is organized as follows. In Sec. II we write down the (SM) effective Hamiltonian for the transition $b \rightarrow s \ell^+ \ell^-$, and recall the available information on the Wilson coefficients. In Sec. III we compute by three-point function QCD sum rules the relevant hadronic quantities for $B \rightarrow K \ell^+ \ell^-$; the same calculation is carried out for $B \rightarrow K^* \ell^+ \ell^-$ in Sec. IV. In Sec. V we study the relations derived by Isgur and Wise [21] and Burdman and Donoghue [22] between rare and semileptonic form factors. Such relations can be worked out in the infinite heavy quark mass limit $m_b \rightarrow \infty$, in the region of maximum momentum transfer t ; a relevant problem is whether they are satisfied also in the low t region, as has been argued by several authors. We investigate this hypothesis and comment on the role of the heavy mass corrections. In Secs. VI and VII we study the transitions $B \rightarrow K \ell^+ \ell^-$ and $B \rightarrow K^* \ell^+ \ell^-$, respectively. Finally, in Sec. VIII we draw our conclusions. Details concerning the calculations are reported in the Appendixes.

II. EFFECTIVE HAMILTONIAN

The effective $\Delta B = -1$, $\Delta S = 1$ Hamiltonian governing in the standard model the rare transition $b \rightarrow s \ell^+ \ell^-$ can be written in terms of a set of local operators [23]:

$$H_W = 4 \frac{G_F}{\sqrt{2}} V_{tb} V_{ts}^* \sum_{i=1}^{10} C_i(\mu) O_i(\mu), \quad (2.1)$$

where G_F is the Fermi constant and V_{ij} are elements of the Cabibbo-Kobayashi-Maskawa (CKM) mixing matrix; we neglect terms proportional to $V_{ub} V_{us}^*$ since the ratio $|V_{ub} V_{us}^* / V_{tb} V_{ts}^*|$ is of the order 10^{-2} . The operators O_i , written in terms of quark and gluon fields, read as

$$\begin{aligned} O_1 &= (\bar{s}_{L\alpha} \gamma^\mu b_{L\alpha}) (\bar{c}_{L\beta} \gamma_\mu c_{L\beta}), \\ O_2 &= (\bar{s}_{L\alpha} \gamma^\mu b_{L\beta}) (\bar{c}_{L\beta} \gamma_\mu c_{L\alpha}), \\ O_3 &= (\bar{s}_{L\alpha} \gamma^\mu b_{L\alpha}) [(\bar{u}_{L\beta} \gamma_\mu u_{L\beta}) + \dots + (\bar{b}_{L\beta} \gamma_\mu b_{L\beta})], \\ O_4 &= (\bar{s}_{L\alpha} \gamma^\mu b_{L\beta}) [(\bar{u}_{L\beta} \gamma_\mu u_{L\alpha}) + \dots + (\bar{b}_{L\beta} \gamma_\mu b_{L\alpha})], \\ O_5 &= (\bar{s}_{L\alpha} \gamma^\mu b_{L\alpha}) [(\bar{u}_{R\beta} \gamma_\mu u_{R\beta}) + \dots + (\bar{b}_{R\beta} \gamma_\mu b_{R\beta})], \\ O_6 &= (\bar{s}_{L\alpha} \gamma^\mu b_{L\beta}) [(\bar{u}_{R\beta} \gamma_\mu u_{R\alpha}) + \dots + (\bar{b}_{R\beta} \gamma_\mu b_{R\alpha})], \\ O_7 &= \frac{e}{16\pi^2} m_b (\bar{s}_{L\alpha} \sigma^{\mu\nu} b_{R\alpha}) F_{\mu\nu}, \\ O_8 &= \frac{g_s}{16\pi^2} m_b \left[\bar{s}_{L\alpha} \sigma^{\mu\nu} \left(\frac{\lambda^a}{2} \right)_{\alpha\beta} b_{R\beta} \right] G_{\mu\nu}^a, \\ O_9 &= \frac{e^2}{16\pi^2} (\bar{s}_{L\alpha} \gamma^\mu b_{L\alpha}) \bar{\ell} \gamma_\mu \ell, \\ O_{10} &= \frac{e^2}{16\pi^2} (\bar{s}_{L\alpha} \gamma^\mu b_{L\alpha}) \bar{\ell} \gamma_\mu \gamma_5 \ell \end{aligned} \quad (2.2)$$

TABLE I. Wilson coefficients $C_i(\mu)$ for $\Lambda_{\overline{\text{MS}}}^{(5)} = 225$ MeV, $\mu = 5$ GeV, and $m_t = 174$ GeV.

	NDR	HV
C_1	-0.243	
C_2	1.105	
C_3	1.083×10^{-2}	
C_4	-2.514×10^{-2}	
C_5	7.266×10^{-3}	
C_6	-3.063×10^{-2}	
C_7	-0.312	
C_9	4.193	3.998
C_{10}	-4.578	

(α, β are color indices, $b_{R,L} = [(1 \pm \gamma_5)/2]b$, and $\sigma^{\mu\nu} = (i/2)[\gamma^\mu, \gamma^\nu]$); e and g_s are the electromagnetic and the strong coupling constants, respectively, and $F_{\mu\nu}$ and $G_{\mu\nu}^a$ in O_7 and O_8 denote the electromagnetic and the gluonic field strength tensors. O_1 and O_2 are current-current operators, and O_3, \dots, O_6 are usually named QCD penguin operators, O_7 (inducing the radiative $b \rightarrow s \gamma$ decay) and O_8 are magnetic penguin operators, O_9 and O_{10} are semileptonic electroweak penguin operators.

The Wilson coefficients $C_i(\mu)$ have been partially computed at next-to-leading order in QCD by several groups [24–26]. As discussed in Ref. [25], in the analysis of $B \rightarrow X_s \ell^+ \ell^-$ at next-to-leading order logarithmic corrections must be consistently included only in the coefficient C_9 , since at the leading approximation O_9 is the only operator responsible for the transition $b \rightarrow s \ell^+ \ell^-$. The contribution of the other operators (excluding O_8 , which, however, is not involved in the processes we are studying) appears only at next-to-leading order, and therefore their Wilson coefficients must be evaluated at the leading approximation.

Following [25] we use in our phenomenological analysis of the decays $B \rightarrow K^{(*)} \ell^+ \ell^-$ (within the standard model) the numerical values of the Wilson coefficients collected in Table I. We choose the scale $\mu = 5$ GeV $\approx m_b$, $\Lambda_{\overline{\text{MS}}}^{(5)} = 225$ MeV, where $\overline{\text{MS}}$ denotes the modified minimal subtraction scheme, and the top quark mass $m_t = 174$ GeV from the measurement of the Collider Detector at Fermilab (CDF) Collaboration [27]. The coefficient C_9 , which is evaluated at the next-to-leading order approximation, displays a dependence on the regularization scheme, as can be observed in Table I comparing the result obtained using the 't Hooft–Veltman (HV) and the naive dimensional regularization (NDR) scheme. Such a dependence must disappear in the decay amplitude if all corrections are taken into account. We shall include in our analysis the uncertainty on C_9 as a part of the theoretical error. In Table I it can also be observed that the coefficients of O_3 – O_6 are small $\sim (10^{-2})$; therefore, the contribution of such operators can be neglected, and the analysis can be carried out considering only the operators O_1, O_2, O_7, O_9 , and O_{10} .

The various extensions of the standard model, such as models involving supersymmetry, multi-Higgs-boson and left-right models, induce two kind of changes in the low energy Hamiltonian (2.1): First, the values of the coefficients C_i are modified as an effect of additional virtual particles in

the loop diagrams describing the $b \rightarrow s$ transition, and, second, new operators can appear in the operator basis, such as operators with different chirality of the quark current with respect to $O_7 - O_{10}$, e.g.,

$$O'_7 = \frac{e}{16\pi^2} m_b (\bar{s}_R \sigma^{\mu\nu} b_L) F_{\mu\nu},$$

$$O'_9 = \frac{e^2}{16\pi^2} (\bar{s}_R \gamma^\mu b_R) \bar{\ell} \gamma_\mu \ell,$$

and

$$O'_{10} = \frac{e^2}{16\pi^2} (\bar{s}_R \gamma^\mu b_R) \bar{\ell} \gamma_\mu \gamma_5 \ell.$$

This rich structure justifies the interest in $B \rightarrow K^{(*)} \ell^+ \ell^-$, where operators of different origin act coherently in determining rates, spectra, and asymmetries. For example, it would be interesting to search for the effects of possible interactions that produce a coefficient C_7 with opposite sign [5,7]. In this work we shall not analyze such new effects, limiting ourselves to studying the above processes within the theoretical framework provided us by the standard model. However, it is worth stressing that our results for the hadronic matrix elements of the operators appearing in (2.1) represent a complete set of quantities also for the analysis of the decays $B \rightarrow K^{(*)} \ell^+ \ell^-$ in a context different from the standard model.

III. FORM FACTORS OF THE DECAY $B \rightarrow K \ell^+ \ell^-$

The matrix elements of the operators O_1 , O_2 , O_7 , O_9 , and O_{10} in Eq. (2.2) between the external states B and K can be parametrized in terms of form factors as

$$\begin{aligned} \langle K(p') | \bar{s} \gamma_\mu b | B(p) \rangle &= (p + p')_\mu F_1(q^2) + \frac{M_B^2 - M_K^2}{q^2} \\ &\times q_\mu [F_0(q^2) - F_1(q^2)] \end{aligned} \quad (3.1)$$

$[q = p - p', F_1(0) = F_0(0)]$ and

$$\begin{aligned} \langle K(p') | \bar{s} i \sigma_{\mu\nu} q^\nu b | B(p) \rangle \\ = [(p + p')_\mu q^2 - (M_B^2 - M_K^2) q_\mu] \frac{F_T(q^2)}{M_B + M_K}. \end{aligned} \quad (3.2)$$

The heavy-to-light meson form factors F_1 and F_0 appear in the calculation of two-body nonleptonic $B \rightarrow KX$ decays, if the factorization approximation is adopted; neglecting $SU(3)_F$ -breaking effects, they govern the semileptonic decay $B \rightarrow \pi \ell^+ \ell^-$.

F_1 and F_0 have already been studied by three-point QCD sum rules [16,28]. In the following we describe in detail the calculation of F_T ; for the sake of completeness, we also report the results for $F_1(q^2)$ and $F_0(q^2)$ using a unique set of parameters and adopting a coherent numerical procedure, in order to have at our disposal a consistent set of form factors.

To compute F_T within the QCD sum rule approach we consider the three-point correlator [11]

$$\begin{aligned} \Pi_{\alpha\mu\nu}(p, p', q) &= i^2 \int dx dy e^{(ip' \cdot y - ip \cdot x)} \\ &\times \langle 0 | T [J_\alpha^K(y) J_{\mu\nu}(0) J_5^B(x)] | 0 \rangle \end{aligned} \quad (3.3)$$

of the flavor-changing quark current $J_{\mu\nu} = \bar{s} i \sigma_{\mu\nu} b$ and of two currents $J_\alpha^K(y)$ and $J_5^B(x)$ with the K and B quantum numbers, respectively: $J_\alpha^K(y) = \bar{q}(y) \gamma_\alpha \gamma_5 s(y)$ and $J_5^B(x) = \bar{b}(x) i \gamma_5 q(x)$. The correlator $\Pi_{\alpha\mu\nu}$ can be expanded in a set of independent Lorentz structures:

$$\Pi_{\alpha\mu\nu} = i p'_\alpha (p_\mu p'_\nu - p_\nu p'_\mu) \Pi + i \sum_n a_{\alpha\mu\nu}^{(n)} \Pi^{(n)}, \quad (3.4)$$

where Π and $\Pi^{(n)}$ are functions of p^2 , p'^2 , and q^2 , and $a_{\alpha\mu\nu}^{(n)}$ are other tensors set up using the vectors p and p' and the metric tensor $g_{\mu\nu}$.

Let us consider Π . To incorporate the quark-hadron duality, on which the QCD sum rule approach is based, we write down for $\Pi(p^2, p'^2, q^2)$ a dispersive representation

$$\begin{aligned} \Pi(p^2, p'^2, q^2) &= \frac{1}{\pi^2} \int_{m_b^2}^{+\infty} ds \int_{m_s^2}^{+\infty} ds' \frac{\rho(s, s', q^2)}{(s - p^2)(s' - p'^2)} \\ &+ \text{subtractions} \end{aligned} \quad (3.5)$$

in the variables p^2 and p'^2 corresponding to the B and K channels, respectively. In the region of low values of s, s' the physical spectral density $\rho(s, s', q^2)$ contains a double δ -function term corresponding to the transition $B \rightarrow K$, and therefore the function Π can be written as

$$\begin{aligned} \Pi &= \frac{R}{(M_B^2 - p^2)(M_K^2 - p'^2)} \\ &+ \frac{1}{\pi^2} \int_D ds ds' \frac{\rho^{\text{had}}(s, s', q^2)}{(s - p^2)(s' - p'^2)}, \end{aligned} \quad (3.6)$$

where the residue R is given in terms of the form factor $F_T(q^2)$ and of the leptonic constants f_K and f_B , defined by the matrix elements $\langle 0 | \bar{q} \gamma_\mu \gamma_5 s | K(p') \rangle = i f_K p'_\mu$ and $\langle 0 | \bar{q} i \gamma_5 b | B(p) \rangle = f_B M_B^2 / m_b$ (we put $m_q = 0$): $R = H F_T(q^2)$ with $H = -2 f_K f_B M_B^2 / m_b (M_B + M_K)$. The integration domain D in (3.6), where higher resonances with the same B and K quantum numbers contribute to the spectral density ρ , starts from two effective thresholds s_0 and s'_0 .

Also the perturbative contribution to Π , computed for $p^2 \rightarrow -\infty$ and $p'^2 \rightarrow -\infty$, can be written as Eq. (3.5). Moreover, considering the first power corrections of the operator product expansion (OPE) of the correlator (3.3) we get the representation

$$\begin{aligned} \Pi(p^2, p'^2, q^2) &= \frac{1}{\pi^2} \int_{m_b^2}^{+\infty} ds \int_{m_s^2}^{+\infty} ds' \frac{\rho^{\text{QCD}}(s, s', q^2)}{(s - p^2)(s' - p'^2)} \\ &+ d_3 \langle \bar{q} q \rangle + d_5 \langle \bar{q} \sigma G q \rangle + \dots \end{aligned} \quad (3.7)$$

$\rho^{\text{QCD}}(s, s', q^2)$ is the perturbative spectral function; the two other terms in (3.7), expressed as a combination of vacuum expectation values of quark and gluon gauge-invariant operators of dimension 3 and 5, respectively, $\langle \bar{q} q \rangle$ and

$\langle \bar{q} \sigma G q \rangle = \langle g_s \bar{q} \sigma^{\mu\nu} G_{\mu\nu}^a (\lambda^a/2) q \rangle$, parametrize the lowest order power corrections. The expressions for ρ^{QCD} and d_5 can be found in Appendix A, Eqs. (A2)–(A4); in this particular case d_3 vanishes.

We now invoke the quark-hadron duality; i.e., we assume that the physical and the perturbative spectral densities are dual to each other, giving the same result when integrated over an appropriate interval. Assuming duality in the region D of the hadronic continuum

$$\int_D ds \, ds' \{ \rho^{\text{had}}(s, s', q^2) - \rho^{\text{QCD}}(s, s', q^2) \} = 0, \quad (3.8)$$

we derive the sum rule for F_T :

$$\begin{aligned} \frac{HF_T(q^2)}{(M_B^2 - p^2)(M_K^2 - p'^2)} &= \frac{1}{\pi^2} \int_{D'} ds \, ds' \frac{\rho^{\text{QCD}}(s, s', q^2)}{(s - p^2)(s' - p'^2)} \\ &\quad + d_3 \langle \bar{q} q \rangle + d_5 \langle \bar{q} \sigma G q \rangle + \dots, \end{aligned} \quad (3.9)$$

where D' is the region corresponding to the low-lying B and K states: $m_b^2 \leq s \leq s_0$, $s'_-(s) \leq s' \leq s'_+(s)$ with

$$\begin{aligned} s'_\pm(s) &= m_s^2 + \frac{(s - m_b^2)}{2m_b^2} [(m_b^2 + m_s^2 - q^2) \\ &\quad \pm \sqrt{(m_b^2 + m_s^2 - q^2)^2 - 4m_b^2 m_s^2}] \end{aligned}$$

and $s'_+ \leq s'_0$. The effective thresholds s_0 and s'_0 can be fixed from the QCD sum rule analysis of two-point functions in the b and s channels. We get s_0 from the calculation of f_B , and s'_0 from the expected mass of the first radial excitation of the kaon.

An improvement of the expression in (3.9) can be obtained by applying to the left- and right-hand sides the Shifman-Vainshtein-Zakharov- (SVZ-) Borel transform, defined by

$$\mathcal{B}_{M^2} \frac{1}{(m^2 - p^2)^n} = \frac{1}{(n-1)!} \frac{e^{-m^2/M^2}}{(M^2)^n}, \quad (3.10)$$

both in the variables $-p^2$ and $-p'^2$; M^2 is a new (Borel) parameter. This operation has the advantage that the convergence of the power series is improved by factorials; moreover, for low values of M^2 and M'^2 the possible contribution of higher states in Eq. (3.9) is exponentially suppressed. The resulting Borel transformed sum rule for F_T reads

$$HF_T(q^2) e^{-M_B^2/M^2 - M_K^2/M'^2} = \frac{1}{\pi^2} \int_{D'} ds \, ds' \rho^{\text{QCD}}(s, s', q^2) e^{-s/M^2 - s'/M'^2} + [\tilde{d}_3 \langle \bar{q} q \rangle + \tilde{d}_5 \langle \bar{q} \sigma G q \rangle] e^{-m_b^2/M^2 - m_s^2/M'^2}. \quad (3.11)$$

From Eq. (3.11) the form factor $F_T(q^2)$ can be derived, once the value of the Borel parameters M^2 and M'^2 is fixed. This can be done observing that, since M^2 and M'^2 are unphysical quantities, F_T must be independent of them (stability region of the sum rule); moreover, the values of M^2 and M'^2 should allow a hierarchical structure in the series of the power correction and a suppression of the contribution of the continuum in the hadronic side of the sum rule.

In our numerical analysis we use the values for the quark condensates (at a renormalization scale $\mu \approx 1$ GeV) [11]:

$$\langle \bar{q} q \rangle = (-230 \text{ MeV})^3,$$

$$\left\langle \bar{q} g_s \sigma^{\mu\nu} G_{\mu\nu}^a \frac{\lambda^a}{2} q \right\rangle = m_0^2 \langle \bar{q} q \rangle, \quad (3.12)$$

with $m_0^2 = 0.8 \text{ GeV}^2$. Notice that the numerical results do not change sensitively if the condensates are evaluated at higher scales using the leading-logarithmic approximation for their anomalous dimension.

As for the quark masses and leptonic constants, we use $m_s = 0.175 \text{ GeV}$, $m_b = 4.6 \text{ GeV}$, $f_K = 0.16 \text{ GeV}$, and $f_B = 0.18 \text{ GeV}$. The thresholds s_0 and s'_0 are chosen in the range $s_0 = (33-36) \text{ GeV}^2$ and $s'_0 = (1.4-1.6) \text{ GeV}^2$, with the Borel parameters kept fixed to the values $M^2 = 8 \text{ GeV}^2$ and $M'^2 = 2 \text{ GeV}^2$.

Putting these parameters in Eq. (3.11) we obtain the form factor F_T depicted in Fig. 1, where the different curves correspond to different choices of the thresholds s_0 and s'_0 . In the sum rule, the perturbative term is a factor of 4–5 times larger than the $D=5$ contribution, and the integral of the spectral function over the region D' gives more than 60% of the result of the integration over the whole region of the dispersion relation (3.5). The duality window, where the results become independent of the Borel parameters M^2 and M'^2 , starts at $M^2 \approx 7 \text{ GeV}^2$ and $M'^2 \approx 1.7 \text{ GeV}^2$; varying M^2 in the range 7–9 GeV^2 and M'^2 in the range 1.7–2.5 GeV^2 the results change within the bounds provided by the different curves depicted in Fig. 1.

The same analysis can be applied to the form factors F_1 and F_0 using the flavor-changing vector current $J_\mu = \bar{s} \gamma_\mu b$ in the correlator (3.3) and studying the projection $q^\mu \Pi_{\alpha\mu}$ to derive F_0 . We report in Appendix A the relevant quantities appearing in the sum rules for F_1 and F_0 ; the difference with respect to [15], as far as F_1 is concerned, is that we keep all terms proportional to powers of the strange quark mass m_s . In the calculation of both the form factors, the contributions of the perturbative term and of the $D=3$ term have comparable size, whereas the $D=5$ term is one order of magnitude smaller; the contribution of the resonance in the hadronic side of the rule is nearly equal to the contribution of the continuum. We obtain the form factors $F_1(q^2)$ and $F_0(q^2)$ depicted in Fig. 1. Also in this case the Borel param-

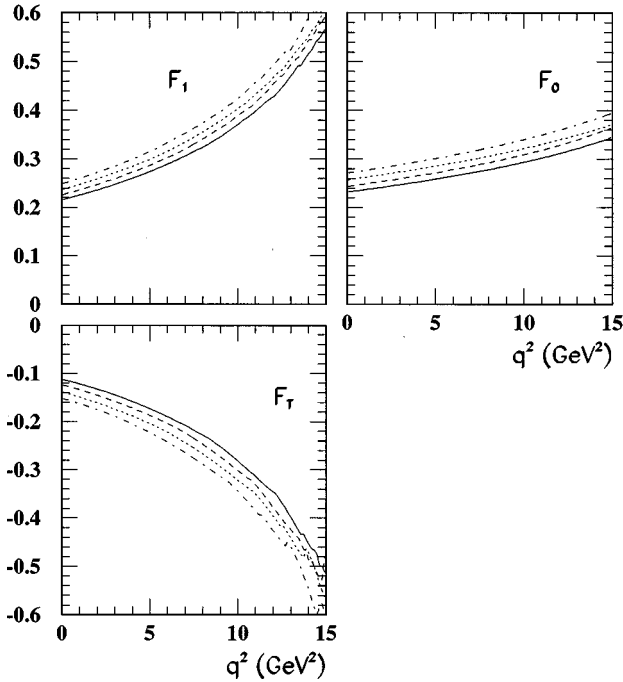


FIG. 1. Form factors $F_1(q^2)$, $F_0(q^2)$, and $F_T(q^2)$ of the transition $B \rightarrow K \ell^+ \ell^-$. The curves refer to different sets of parameters: $s_0 = 33 \text{ GeV}^2$ and $s'_0 = 1.4 \text{ GeV}^2$ (solid line), $s_0 = 33 \text{ GeV}^2$ and $s'_0 = 1.6 \text{ GeV}^2$ (dashed line), $s_0 = 36 \text{ GeV}^2$ and $s'_0 = 1.4 \text{ GeV}^2$ (dotted line), $s_0 = 36 \text{ GeV}^2$ and $s'_0 = 1.6 \text{ GeV}^2$ (dashed-dotted line). The Borel parameters are fixed to $M^2 = 8 \text{ GeV}^2$, $M'^2 = 2 \text{ GeV}^2$.

eters can be varied in the range $M^2 = 7\text{--}9 \text{ GeV}^2$ and $M'^2 = 1.7\text{--}2.5 \text{ GeV}^2$; the results change within the region corresponding to the different curves depicted in Fig. 1 for each form factor.

We observe a different q^2 dependence for the various form factors. In the range of q^2 we are considering ($0 \leq q^2 \leq 13\text{--}15 \text{ GeV}^2$) F_1 follows a simple pole formula:

$$F(q^2) = \frac{F(0)}{1 - \frac{q^2}{M_P^2}}, \quad (3.13)$$

with $F_1(0) = 0.25 \pm 0.03$ and $M_{P_1} \approx 5 \text{ GeV}$. A fit to the formula (3.13) for F_0 gives the result $M_{P_0} \approx 7 \text{ GeV}$. The same formula, applied to F_T , would give $F_T \approx -0.14$ and $M_P \approx 4.5 \text{ GeV}$. Therefore, only the dependence of the form factor $F_1(q^2)$ does not contradict the polar behavior dominated by B_s^* , which is the nearest singularity in the t channel, as we would expect by invoking the vector meson dominance (VMD) ansatz. The form factor F_0 increases softly with q^2 and, as already observed in [28], the fitted mass of the pole is larger than the expected mass of the physical singularity, in this case the $J^P = 0^+ b\bar{s}$ state. As for F_T , the VMD ansatz would predict a polar dependence, with the pole represented by B_s^* ; on the other hand, we observe that F_T can be related to F_1 and F_0 by an identity obtained by the equation of motion:

$$F_T(q^2) = (M_B + M_K)(m_b + m_s) \frac{F_0(q^2) - F_1(q^2)}{q^2}; \quad (3.14)$$

Eq. (3.14) is in agreement with the computed form factor F_T displayed in Fig. 1, and therefore we can use the double pole model:

$$F_T(q^2) = \frac{F_T(0)}{\left(1 - \frac{q^2}{M_{P_1}^2}\right) \left(1 - \frac{q^2}{M_{P_0}^2}\right)}, \quad (3.15)$$

with $F_T(0) = -0.14 \pm 0.03$ and M_{P_1} and M_{P_0} given by the fitted values of the mass of the poles of F_1 and F_0 , respectively.

It is interesting to observe that information on the possible form of the q^2 dependence of the form factors can be derived by studying the limit $m_b \rightarrow \infty$. In this limit, at the zero recoil point where the kaon is at rest in the B meson rest frame, it is straightforward to show that the parametric dependence of the form factors on the heavy meson mass M_B is given by $F_1(q_{\text{max}}^2) \sim \sqrt{M_B}$ and $F_0(q_{\text{max}}^2) \sim 1/\sqrt{M_B}$ [21]. Both these scaling laws are compatible with the constraint $F_1(0) = F_0(0)$ and with a multipolar functional dependence

$$F_i(q^2) = \frac{F_i(0)}{\left(1 - \frac{q^2}{M_{P_i}^2}\right)^{n_i}} \quad (3.16)$$

if $n_1 = n_0 + 1$. Thus, in the limit $m_b \rightarrow \infty$, to a polar form factor $F_1(q^2)$ corresponds a nearly constant form factor $F_0(q^2)$. The outcome of QCD sum rules is in agreement with this observation [29]; the observed increasing of F_0 would be due to subleading terms contributing at finite m_b .

Let us now compare our results with the outcome of different QCD-based approaches. In the channel $B \rightarrow \pi$ the form factor F_1 has been computed by light-cone sum rules [30], with numerical results in agreement, at finite b -quark mass, with the outcome of three-point function sum rules.

As for lattice QCD, both F_1 and F_0 have been computed at large q^2 [31], and data show that F_0 has a flat dependence on the momentum transfer, whereas F_1 increases with q^2 .

The full set of form factors F_1 , F_0 , and F_T by these other methods is still missing; the complete comparison of our results with such different approaches could help in understanding the drawbacks and the advantages of the various methods; this would shed light on the issue of decays such as $B \rightarrow \pi \ell^+ \ell^-$ that are of interest as far as the measurement of V_{ub} is concerned.

IV. FORM FACTORS OF $B \rightarrow K^* \ell^+ \ell^-$

The form factors parametrizing the hadronic matrix elements of the transition $B \rightarrow K^* \ell^+ \ell^-$ can also be computed by QCD sum rules by considering a three-point correlator with the interpolating current for K^* represented by the vector current $J_\alpha^{K^*}(y) = \bar{q}(y) \gamma_\alpha s(y)$. Let us define the $B \rightarrow K^*$ matrix elements:

$$\begin{aligned} \langle K^*(p', \epsilon) | \bar{s} \gamma_\mu (1 - \gamma_5) b | B(p) \rangle = & \epsilon_{\mu\nu\alpha\beta} \epsilon^{*\nu} p^\alpha p'^\beta \frac{2V(q^2)}{M_B + M_{K^*}} - i \left[\epsilon_\mu^* (M_B + M_{K^*}) A_1(q^2) - (\epsilon^* \cdot q)(p + p')_\mu \frac{A_2(q^2)}{(M_B + M_{K^*})} \right. \\ & \left. - (\epsilon^* \cdot q) \frac{2M_{K^*}}{q^2} [A_3(q^2) - A_0(q^2)] q_\mu \right] \end{aligned} \quad (4.1)$$

and

$$\begin{aligned} \left\langle K^*(p', \epsilon) \left| \bar{s} \sigma_{\mu\nu} q^\nu \frac{(1 + \gamma_5)}{2} b \right| B(p) \right\rangle = & i \epsilon_{\mu\nu\alpha\beta} \epsilon^{*\nu} p^\alpha p'^\beta 2T_1(q^2) + [\epsilon_\mu^* (M_B^2 - M_{K^*}^2) - (\epsilon^* \cdot q)(p + p')_\mu] T_2(q^2) \\ & + (\epsilon^* \cdot q) \left[q_\mu - \frac{q^2}{M_B^2 - M_{K^*}^2} (p + p')_\mu \right] T_3(q^2). \end{aligned} \quad (4.2)$$

A_3 can be written as a linear combination of A_1 and A_2 :

$$A_3(q^2) = \frac{M_B + M_{K^*}}{2M_{K^*}} A_1(q^2) - \frac{M_B - M_{K^*}}{2M_{K^*}} A_2(q^2), \quad (4.3)$$

with the condition $A_3(0) = A_0(0)$. The identity $\sigma_{\mu\nu} \gamma_5 = -(i/2) \epsilon_{\mu\nu\alpha\beta} \sigma^{\alpha\beta}$ ($\epsilon_{0123} = +1$) implies that $T_1(0) = T_2(0)$.

The form factors $T_1(q^2)$ and $T_2(q^2)$ can be derived by the correlator

$$\begin{aligned} \tilde{\Pi}_{\alpha\mu}(p, p', q) = & i^2 \int dx dy e^{(ip' \cdot y - ip \cdot x)} \\ & \times \langle 0 | T[J_\alpha^{K^*}(y) \tilde{J}_\mu(0) J_5^B(x)] | 0 \rangle, \end{aligned} \quad (4.4)$$

with

$$\tilde{J}_\mu = \bar{s} \sigma_{\mu\nu} \frac{1 + \gamma_5}{2} q^\nu b.$$

Expanding $\tilde{\Pi}_{\alpha\mu}$ in Lorentz-independent structures

$$\tilde{\Pi}_{\alpha\mu} = i \epsilon_{\alpha\mu\rho\beta} p^\rho p'^\beta \tilde{\Pi}_1 + g_{\alpha\mu} \tilde{\Pi}_2 + \text{other structures in } p, p', \quad (4.5)$$

we get T_1 and T_2 from $\tilde{\Pi}_1$ and $\tilde{\Pi}_2$, respectively. The sum rules have the same structure as that of Eqs. (3.9), (3.11), with the perturbative spectral functions $\rho(s, s', q^2)$ and the power corrections d_3 and d_5 reported in Appendix B. The only difference with respect to the kaon case is the value of the K^* leptonic constant, defined by the matrix element $\langle 0 | \bar{q} \gamma_\mu s | K^*(p, \epsilon) \rangle = f_{K^*} M_{K^*} \epsilon_\mu$, with $f_{K^*} = 216$ MeV.

In Fig. 2 we depict the form factors $T_1(q^2)$ and $T_2(q^2)$ obtained choosing the threshold s'_0 in the range 1.6–1.8 GeV^2 and the other parameters as in the previous section. In the sum rule for both the form factors the perturbative term does not dominate over the nonperturbative ones: At $q^2=0$ it represents 30% of the quark condensate contribution, and is nearly equal to the $D=5$ term. However, it rapidly increases with the momentum transfer, and at $q^2=15 \text{ GeV}^2$ it is equal to the contribution of the $D=3$ term, whereas the $D=5$ contribution is an order of magnitude smaller.

Concerning the form factor T_3 , we observe that it contributes, together with T_1 and T_2 , to other invariant functions in (4.5) and, in principle, it also could be obtained by a sum rule. However, since it can be related to A_1 , A_2 , and A_0 by applying the equation of motion,

$$T_3(q^2) = M_{K^*} (m_b - m_s) \frac{A_3(q^2) - A_0(q^2)}{q^2}; \quad (4.6)$$

we prefer to use this expression to determine it, considering that this procedure is successful for $F_T(q^2)$.

The form factors V and A_i can be obtained by studying the correlator (4.4) with a vector $J_\mu^V = \bar{s} \gamma_\mu b$ and an axial

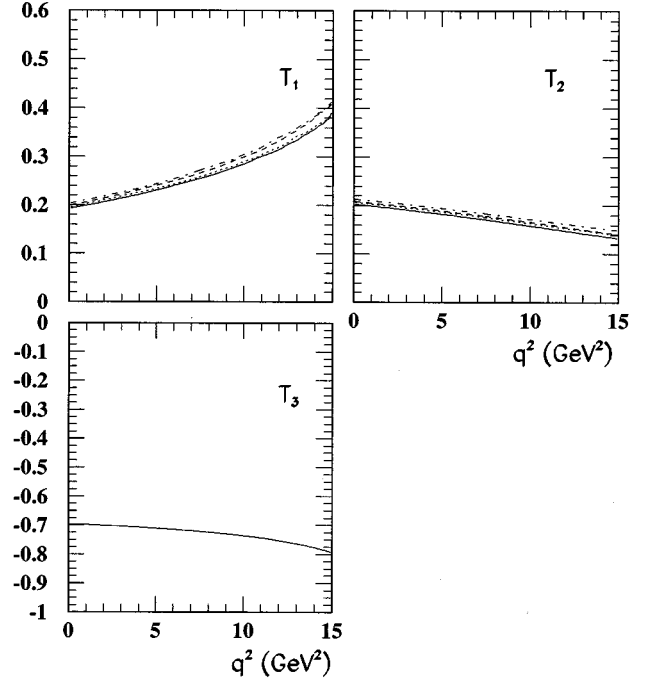


FIG. 2. Form factors $T_1(q^2)$, $T_2(q^2)$, and $T_3(q^2)$ of the transition $B \rightarrow K^* \ell^+ \ell^-$. The curves refer to different sets of parameters: $s_0 = 33 \text{ GeV}^2$ and $s'_0 = 1.6 \text{ GeV}^2$ (solid line), $s_0 = 33 \text{ GeV}^2$ and $s'_0 = 1.8 \text{ GeV}^2$ (dashed line), $s_0 = 36 \text{ GeV}^2$ and $s'_0 = 1.6 \text{ GeV}^2$ (dotted line), $s_0 = 36 \text{ GeV}^2$ and $s'_0 = 1.8 \text{ GeV}^2$ (dashed-dotted line). The Borel parameters are fixed to $M^2 = 8 \text{ GeV}^2$, $M'^2 = 2 \text{ GeV}^2$.

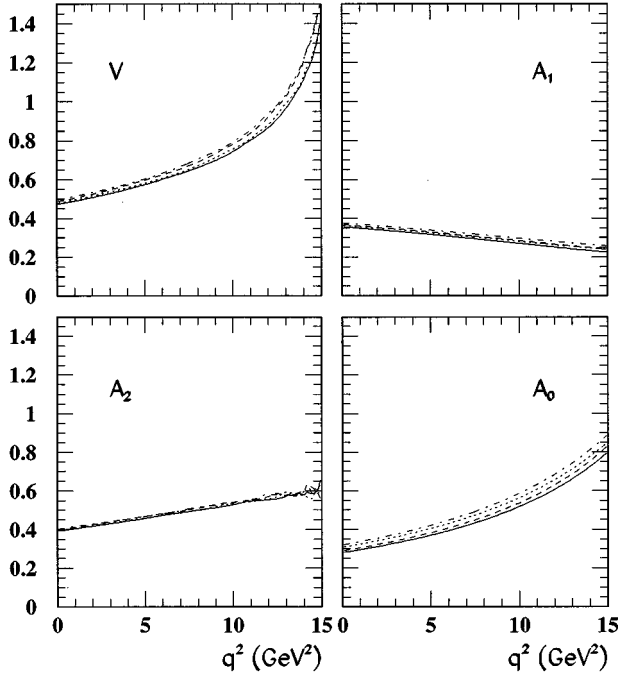


FIG. 3. Form factors $V(q^2)$, $A_1(q^2)$, $A_2(q^2)$, and $A_0(q^2)$ of $B \rightarrow K^* \ell^+ \ell^-$. The curves refer to the same set of parameters as in Fig. 2.

$J_\mu^A = \bar{s} \gamma_\mu \gamma_5 b$ flavor-changing current, considering the projection $q^\mu J_\mu^A$ to derive A_0 . We collect in Appendix B the complete expressions appearing in the relevant sum rules for all the form factors, excluding A_0 , whose expressions can be found in [32]; also in this case the difference with respect to [15] is that we include all powers of the strange quark mass.

Using our set of parameters we get $V(q^2)$, $A_1(q^2)$, $A_2(q^2)$, and $A_0(q^2)$ depicted in Fig. 3, and, using (4.6), the form factor T_3 in Fig. 2.

As happens for T_1 and T_2 , also in the sum rules for V , A_1 , and A_2 the perturbative term, at $q^2=0$, is smaller than the $D=3$ contribution; the relative weights of the various contributions change with the momentum transfer, and at $q^2=15 \text{ GeV}^2$ the $D=0$ and $D=3$ terms have comparable size. As it happens for the $B \rightarrow K$ form factors, the chosen values of M^2 and M'^2 , $M^2=8 \text{ GeV}^2$ and $M'^2=2 \text{ GeV}^2$, are within the duality window where the results are independent of the Borel parameters. Also in this case, varying M^2 and M'^2 in the ranges $M^2=7-9 \text{ GeV}^2$ and $M'^2=1.7-2.5 \text{ GeV}^2$, the final results change within the same uncertainty coming from the variation of the continuum threshold.

Considering the results displayed in Figs. 2 and 3, we collect the form factors T_i , V , and A_i in three sets, according to their functional dependence on the momentum transfer. In the first set we include T_1 , V , and A_0 , which display a sharp increase with q^2 . It is possible to fit them with a polar q^2 dependence, Eq. (3.13) (as observed also in [16,32]), with $T_1(0)=0.19 \pm 0.03$ and $M_P \approx 5.3 \text{ GeV}$, $V(0)=0.47 \pm 0.03$ and $M_P \approx 5 \text{ GeV}$, and $A_0(0)=0.30 \pm 0.03$ and $M_P \approx 4.8 \text{ GeV}$ [the difference with respect to the value $T_1(0)=0.17 \pm 0.03$

TABLE II. Parameters of the form factors. The functional q^2 dependence is either polar, $F(q^2)=F(0)/(1-q^2/M_P^2)$, or linear, $F(q^2)=F(0)(1+\beta q^2)$. For the form factor F_T see text.

	$F(0)$	$M_P \text{ (GeV)}$	$\beta \text{ (GeV}^{-2}\text{)}$
F_1	0.25 ± 0.03	5	
F_0	0.25 ± 0.03	7	
F_T	-0.14 ± 0.03		
V	0.47 ± 0.03	5	
A_1	0.37 ± 0.03		-0.023
A_2	0.40 ± 0.03		0.034
A_0	0.30 ± 0.03	4.8	
T_1	0.19 ± 0.03	5.3	
T_2	0.19 ± 0.03		-0.02
T_3	-0.7		0.005

in Ref. [17] is due to the effect of the strange quark mass, which here has been included].

The error in the mass of the pole is correlated to the error in the form factor at $q^2=0$, and it can be estimated to be of the order of 200–300 MeV. The relevant result is that the masses of the poles are not far from the values expected by the dominance of the nearest singularity in the t channel: $M_P=M_{B_s^*}$ for T_1 and V , $M_P=M_{B_s}$ for A_0 . We stress that the fit is performed in a range of values of q^2 where the QCD calculation can be meaningfully carried out, therefore large momenta transferred ($q^2 > 15 \text{ GeV}^2$) are not taken into account.

In the second set of form factors we include T_2 , T_3 , and A_1 . They softly decrease with q^2 : $F_i(q^2)=F_i(0)(1+\beta q^2)$, with $T_2(0)=T_1(0)$ and $\beta=-0.02 \text{ GeV}^{-2}$, $T_3(0)=-0.7$ and $\beta=0.005 \text{ GeV}^{-2}$, and $A_1(0)=0.37 \pm 0.03$ and $\beta=-0.023 \text{ GeV}^{-2}$ with the error in β at the level of 10%. The dependence of T_3 is related to A_1 , A_2 , and A_0 .

The last form factor A_2 linearly increases with q^2 : $A_2(0)=0.40 \pm 0.03$ and $\beta=0.034 \text{ GeV}^{-2}$. A fit to a polar dependence for this form factor would give $M_P \geq 7 \text{ GeV}$ for the mass of the pole.

The parameters of all the form factors are collected in Table II. Albeit the form factors have been computed in a well-defined range of momentum transfer, once their functional q^2 dependence has been fitted and the parameters determined, we extrapolate them up to q_{max}^2 . This procedure cannot be avoided within the method of QCD sum rules, where large positive values of q^2 are not accessible since there is a region where the distance between the points x , y , and 0 in the correlator, which is the initial ingredient of this approach, is large, and therefore the standard OPE cannot be used; this is shown by the occurrence of singularities in the correlator when q^2 is close to q_{max}^2 .

As for the computed dependence on the momentum transfer, is worth remembering that deviations from the VMD expectations for the form factors A_1 and A_2 have been already observed in the literature, first in the $D \rightarrow K^* \ell^+ \ell^-$ [15] channel and then for $B \rightarrow \rho \ell^+ \ell^-$ [16]. Here we find a kind of common feature; i.e., all form factors deviating from the po-

lar dependence (excluding F_T) seem to depend linearly on the momentum transfer, with small (positive or negative) slopes.

It is interesting that also for $T_1(q^2)$ and $T_2(q^2)$ we can use the argument developed in the previous section concerning the limit $m_b \rightarrow \infty$: Since $T_1(q_{\max}^2) \sim \sqrt{M_B}$ and $T_2(q_{\max}^2) \sim 1/\sqrt{M_B}$, the constraint $T_1(0) = T_2(0)$ can be fulfilled by a multipolar q^2 dependence if $n_1 = n_2 + 1$ in Eq. (3.16).

At zero momentum transfer our results numerically agree with those obtained by the method of light-cone sum rules [33], within the errors and taking into account the different choices of the input parameters. In [33] it has also been observed that T_1 , V , and A_1 have different functional dependences on q^2 ; the difference with respect to our case is that the slopes are larger than those obtained from three-point sum rules; in particular, the form factor A_1 increases with q^2 . The origin of this discrepancy should be investigated.

The form factors T_1 and T_2 have been computed by lattice QCD [34,35] near the point of zero recoil and for the mass of the heavy quark smaller than m_b , due to the finite size of the available lattices; therefore, the results at $q^2 = 0$ and for a realistic value of m_b are obtained after an extrapolation in the momentum transfer and in the heavy quark mass. Also, in this case, in the region of large values of q^2 , the form factor T_1 increases rapidly with the momentum transfer, whereas T_2 is quite flat. As for the analytic q^2 behavior obtained from lattice calculations, it seems to us that larger lattices are needed to enlarge the range of momentum transfer where the measurements can be performed, in order to clearly disentangle different possible dependences of T_1 and T_2 (e.g., dipole versus pole or pole versus constant).

V. RELATIONS BETWEEN RARE AND SEMILEPTONIC B DECAY FORM FACTORS

In the limit $m_b \rightarrow \infty$ Isgur and Wise [21] and Burdman and Donoghue [22] have derived exact relations between the form factors F_T , T_i in Eqs. (3.2), (4.2) and the form factors F_i , V , A_i in Eqs. (3.1), (4.1). These relations can be easily worked out observing that, in the effective theory where the b -quark mass is taken to the infinity, the equation $\gamma^0 b = b$ is satisfied in the rest frame of the B meson.

In our parametrization such relations can be written as follows, near the point of zero recoil [$q^2 \simeq q_{\max}^2 = (M_B - M_{K^*})^2$]:

$$F_T(q^2) = -\frac{M_B + M_K}{2M_B} \left[F_1(q^2) - (M_B^2 - M_K^2) \frac{F_0(q^2) - F_1(q^2)}{q^2} \right], \quad (5.1)$$

$$T_1(q^2) = \frac{M_B + M_{K^*}}{4M_B} A_1(q^2) + \frac{M_B^2 - M_{K^*}^2 + q^2}{4M_B(M_B + M_{K^*})} V(q^2), \quad (5.2)$$

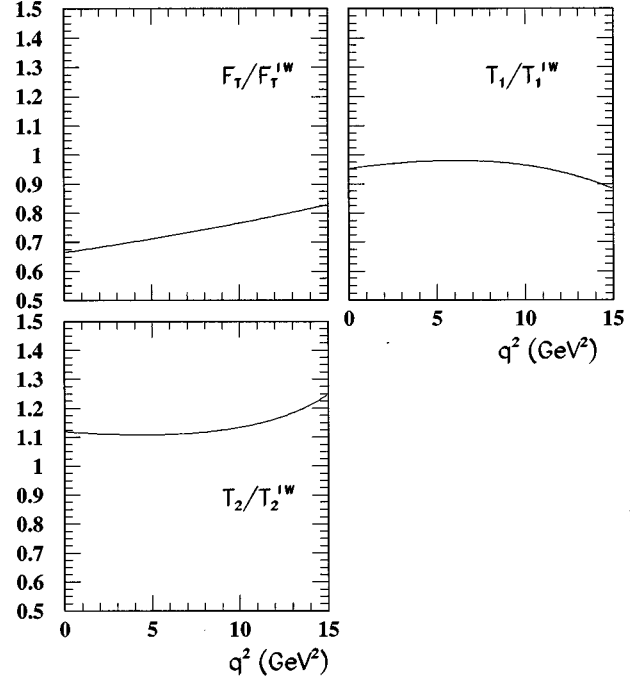


FIG. 4. Momentum dependence of the ratio between rare and semileptonic form factors $\mathcal{R} = F_i(q^2)/F_i^{\text{IW}}(q^2)$; F_i^{IW} are obtained from Eqs. (5.1)–(5.3).

$$T_2(q^2) = \frac{(M_B^2 - M_{K^*}^2 + q^2)}{4M_B(M_B - M_{K^*})} A_1(q^2) + \frac{\lambda(M_B^2, M_{K^*}^2, q^2)}{4M_B(M_B - M_{K^*})(M_B + M_{K^*})^2} V(q^2), \quad (5.3)$$

$$T_3(q^2) = -\frac{M_B^2 + 3M_{K^*}^2 - q^2}{4M_B(M_B + M_{K^*})} V(q^2) + \frac{M_{K^*}}{2M_B} A_3(q^2) + \frac{M_{K^*}(M_B^2 - M_{K^*}^2)}{2M_B} \frac{A_3(q^2) - A_0(q^2)}{q^2}, \quad (5.4)$$

where λ is the triangular function.

It has been argued by several authors that the relations (5.1)–(5.4) could also be valid at low values of q^2 [22], although a general proof has not been found in support of this hypothesis.

Using the form factors computed by QCD sum rules in the previous sections, it is possible to check Eqs. (5.1)–(5.4). In Fig. 4 we plot the ratio $\mathcal{R} = F/F^{\text{IW}}$ in the case of F_T , T_1 , and T_2 , as a function of q^2 , in the range of momentum transfer where the calculation has been carried out. We observe that the relations between the various form factors are verified at different levels of accuracy.

In the case of F_T the ratio \mathcal{R} differs from unity at the level of (25–30)%, including the uncertainty coming from the errors of the various parameters. In particular, at $q^2 = 0$ we have $F_T/F_T^{\text{IW}} = 0.7 \pm 0.1$. The situation is different for the

ratios concerning T_1 and T_2 , which differ from unity at the level of (10–20)%: at $q^2=0$ we have $T_1/T_1^{\text{IW}}=0.94\pm 0.05$ and $T_2/T_2^{\text{IW}}=1.12\pm 0.05$.

These results support the argument put forward in [17] on the validity of the Isgur-Wise relations, in the limit $m_b \rightarrow \infty$ also at small values of q^2 ; they also can be well compared to the outcome of light-cone sum rules, obtained for T_1 at a finite m_b [33]. The conclusion is that the b quark is near to the mass shell also when the recoil of the light hadron is large with respect to m_b , with $1/m_b$ corrections that do not appear to overwhelm the effect.

Relations (5.1)–(5.4) could be used to perform a model-independent analysis of the decays $B \rightarrow K^{(*)} \ell^+ \ell^-$ employing experimental information (when available) on the form factors of the semileptonic transition $B \rightarrow \rho \ell \nu$ [36]. In particular, since (5.1)–(5.4) are valid on general grounds in the large q^2 region, it has been proposed to perform the analysis in the range of large invariant mass of the lepton pair, e.g., $M_{\ell^+ \ell^-} \geq 4$ GeV.

Albeit in principle correct, we feel that, from the experimental point of view, the procedure of extracting the semileptonic $B \rightarrow \rho$ form factors near zero recoil will be rather

difficult, with large uncertainties in the final result. The problem is not avoided by the possible choice of using the form factors of the semileptonic transition $D \rightarrow K^* \ell^+ \nu$, and then rescaling them according to their leading dependence on the heavy mass, i.e.,

$$\frac{V^{B\rho}(q_{\text{max}}^2)}{V^{DK^*}(q_{\text{max}}^2)} = \sqrt{\frac{M_B}{M_D}},$$

etc. [neglecting $\text{SU}(3)_F$ and α_s corrections]. As a matter of fact, in such a procedure the next-to-leading mass corrections could be large and not under control. Finally, as we shall see in the next section, the differential branching ratios of $B \rightarrow K^{(*)} \ell^+ \ell^-$ at large q^2 are small, and therefore the experimental errors are expected to be sizable. For this reason we prefer to propose an analysis of the decay extended to the full range of q^2 , using hadronic quantities determined in a well-defined theoretical framework. The dependence on the computational scheme will be reduced once the different form factors have been computed by different QCD calculations, and the whole information collected in a unique set of form factors.

VI. DECAY $B \rightarrow K \ell^+ \ell^-$

We can now compute the invariant-mass-squared distribution of the lepton pair in the decay $B \rightarrow K \ell^+ \ell^-$:

$$\begin{aligned} \frac{d\Gamma}{dq^2}(B \rightarrow K \ell^+ \ell^-) &= \frac{M_B^3 G_F^2 \alpha^2}{1536 \pi^5} |V_{ts}^* V_{tb}|^2 \left\{ \left| C_7 2m_b \left(-\frac{F_T(q^2)}{M_B + M_K} \right) + C_9^{\text{eff}} F_1(q^2) \right|^2 + |C_{10} F_1(q^2)|^2 \right\} \\ &\times \left[\left(1 - \frac{M_K^2}{M_B^2} \right)^2 + \left(\frac{q^2}{M_B^2} \right)^2 - 2 \left(\frac{q^2}{M_B^2} \right) \left(1 + \frac{M_K^2}{M_B^2} \right) \right]^{3/2} \end{aligned} \quad (6.1)$$

($q^2 = M_{\ell^+ \ell^-}^2$). The contribution of the operators O_7 , O_9 , and O_{10} is taken into account in the terms proportional to C_7 , C_9 , and C_{10} . The operators O_1 and O_2 provide a short distance contribution, with a loop of charm quarks described by the function $h(x, s)$ ($x = m_c/m_b$, $s = q^2/m_b^2$) [23,24]:

$$h(x, s) = - \left[\frac{4}{9} \ln x^2 - \frac{8}{27} - \frac{16}{9} \frac{x^2}{s} + \frac{4}{9} \sqrt{\frac{4x^2}{s} - 1} \left(2 + \frac{4x^2}{s} \right) \arctan \left(\frac{4x^2}{s} - 1 \right)^{-1/2} \right] \quad (6.2)$$

if $s < 4x^2$ and

$$h(x, s) = - \left\{ \frac{4}{9} \ln x^2 - \frac{8}{27} - \frac{16}{9} \frac{x^2}{s} + \frac{2}{9} \sqrt{1 - \frac{4x^2}{s}} \left(2 + \frac{4x^2}{s} \right) \left[\ln \left| \frac{1 + \sqrt{1 - 4x^2/s}}{1 - \sqrt{1 - 4x^2/s}} \right| - i\pi \right] \right\} \quad (6.3)$$

if $s > 4x^2$; the imaginary part in (6.3) comes from on-shell charm quarks. O_1 and O_2 also provide a long distance contribution, related to $c\bar{c}$ bound states ($J/\psi, \psi'$) converting into the lepton pair $\ell^+ \ell^-$ [37,38]. This contribution can be described in terms of the J/ψ and ψ' leptonic decay constants $\langle 0 | \bar{c} \gamma^\mu c | \psi_i(\epsilon, q) \rangle = \epsilon^\mu f_{\psi_i} M_{\psi_i}$ and of the full J/ψ and ψ' decay widths Γ_{ψ_i} . We derive f_{ψ_i} from the experimental branching ratio $\psi_i \rightarrow \ell^+ \ell^-$; in this way the whole contribution of O_1 and O_2 can be taken into account by modifying the coefficient C_9 into C_9^{eff} :

$$\begin{aligned} C_9^{\text{eff}} &= C_9 + (3C_1 + C_2) \left[h(x, s) \right. \\ &\quad \left. + k \sum_{i=1}^2 \frac{\pi \Gamma(\psi_i \rightarrow \ell^+ \ell^-) M_{\psi_i}}{q^2 - M_{\psi_i}^2 + i M_{\psi_i} \Gamma_{\psi_i}} \right]. \end{aligned} \quad (6.4)$$

If the nonleptonic $B \rightarrow K \psi_i$ transition is computed by factorization, the parameter k is given by

$$k = \frac{3}{\alpha^2} \frac{|V_{cb}^* V_{cs}|}{|V_{ts}^* V_{tb}|};$$

the sign between the short distance and the long distance terms in (6.4) can be fixed according to the analyses in Ref. [38]. In Ref. [5] the value of k is appropriately chosen in order to reproduce the quantity

$$B(B \rightarrow K \ell^+ \ell^-)|_{\text{res}} = \sum_{i=1}^2 B(B \rightarrow \psi_i K) B(\psi_i \rightarrow \ell^+ \ell^-) \approx 7 \times 10^{-5} \quad [39]. \quad (6.5)$$

This can be done by choosing $k \approx (1.5-2)(3/\alpha^2)$. Notice that, since the J/ψ and ψ' resonances are narrow, their contribution modifies the dilepton spectrum only in the region close to $M_{\ell^+ \ell^-}^2 = M_{J/\psi}^2, M_{\psi'}^2$.

As input parameters we choose the ratio $m_c/m_b = 0.27-0.29$ and the value of the CKM matrix element $|V_{ts}| \approx 0.04$; a different value for $|V_{ts}|$ only modifies the prediction of the branching ratio, leaving unchanged the shape of the spectrum [40].

We depict in Fig. 5 the obtained invariant-mass-squared distribution of the lepton pair in $B \rightarrow K \ell^+ \ell^-$. In the same figure we also plot the spectrum obtained considering only the short distance contribution, which gives the branching ratio (using $\tau_B = 1.5 \times 10^{-12}$ sec for the B^- meson lifetime) $B(B \rightarrow K \ell^+ \ell^-)|_{sd} \approx 3 \times 10^{-7} |V_{ts}/0.04|^2$, to be compared to the experimental upper limit (obtained excluding the region near J/ψ and ψ') $B(B^- \rightarrow K^- \mu^+ \mu^-) < 0.9 \times 10^{-5}$ (at 90% C.L.) [41,42]. The uncertainty coming from the two possible values of C_9 in Table I is less than 1% and does not have relevant consequences on the predicted branching ratio and on the invariant mass distribution.

From the experimental point of view, the measurement of the spectrum in Fig. 5 is a nontrivial task; hopefully, it will be possible to obtain experimental results from the future dedicated $e^+ e^-$ colliders. The important point to be stressed is that, in the distribution depicted in Fig. 5 the theoretical uncertainty connected to the hadronic matrix element is reduced to a well-defined QCD computational scheme (QCD sum rules), so that in the studies of the effects of interactions beyond the standard model the hadronic uncertainty no longer plays a major role.

VII. DECAY $B \rightarrow K^* \ell^+ \ell^-$

A great deal of information can be obtained from the channel $B \rightarrow K^* \ell^+ \ell^-$ investigating, together with the lepton invariant mass distribution, also the forward-backward (FB) asymmetry in the dilepton angular distribution; this may reveal effects beyond the standard model that could not be observed in the analysis of the decay rate.

A FB asymmetry in the dilepton angular distribution is a hint on parity violation. Since the decay $B \rightarrow K^* \ell^+ \ell^-$ proceeds through γ , Z , and W intermediate bosons, we expect a different behavior in the various q^2 kinematical regions. In the region of low q^2 , the photon exchange dominates, leading to a substantially vectorlike parity-conserving interaction; as a consequence, we expect a small asymmetry. On the other hand, when q^2 is large, the contribution of Z and W

exchange diagrams becomes important, and the interaction acquires the $V-A$ parity-violating structure, leading to a large asymmetry. As already observed in Ref. [43] this pattern strongly depends on the value of the top quark mass, and the penguin diagrams with Z exchange and the W box diagram are expected to overwhelm the photon penguin diagram in correspondence to the measured m_t . Moreover, since the FB asymmetry is sensitive not only to the magnitude of the Wilson coefficients, but also to their sign [5], it can be used to probe the values predicted by the standard model.

Let us define θ_ℓ as the angle between the ℓ^+ direction and the B direction in the rest frame of the lepton pair. Since, in the case of massless leptons, as we assume, the amplitude can be written as sum of noninterfering helicity amplitudes, the double differential decay rate reads as follows:

$$\frac{d^2\Gamma}{dq^2 d\cos\theta_\ell} = \frac{G_F^2 |V_{tb} V_{ts}^*|^2 \alpha^2 \lambda^{1/2}(M_B^2, M_{K^*}^2, q^2)}{2^{13} \pi^5} \frac{1}{M_B^3} \times \{ \sin^2 \theta_\ell A_L + q^2 [(1 + \cos \theta_\ell)^2 (A_+^L + A_-^R) + (1 - \cos \theta_\ell)^2 (A_-^L + A_+^R)] \}, \quad (7.1)$$

where A_L corresponds to a longitudinally polarized K^* , while $A_{+(-)}^{L(R)}$ represent the contribution from left (right) leptons and from K^* with transverse polarization:

$$\epsilon_\pm = \left(0, \frac{1}{\sqrt{2}}, \pm \frac{i}{\sqrt{2}}, 0 \right).$$

We obtain

$$A_L = \frac{1}{M_{K^*}^2} \{ |B_1(M_B^2 - M_{K^*}^2 - q^2) + B_2 \lambda|^2 + |D_1(M_B^2 - M_{K^*}^2 - q^2) + D_2 \lambda|^2 \} \quad (7.2)$$

and

$$A_\pm^L = |\lambda^{1/2}(A - C) \mp (B_1 - D_1)|^2, \quad (7.3)$$

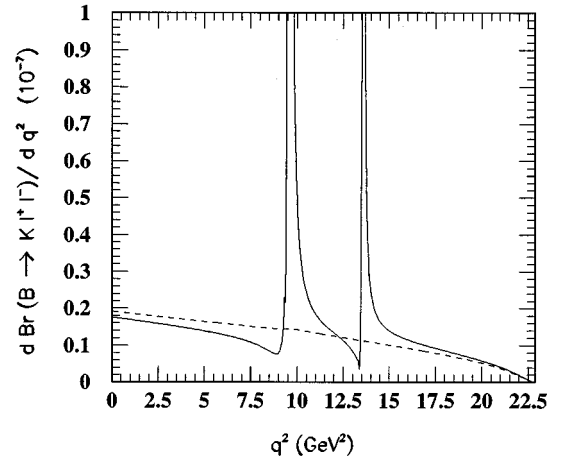


FIG. 5. Invariant-mass-squared distribution of the lepton pair for the decay $B \rightarrow K \ell^+ \ell^-$; the dashed line refers to the short distance contribution only.

$$A_{\pm}^R = |\lambda^{1/2}(A+C) \mp (B_1+D_1)|^2, \quad (7.4)$$

where $\lambda = \lambda(M_B^2, M_{K^*}^2, q^2)$. The terms A, C, B_1, D_1 contain the short distance coefficients, as well as the form factors:

$$A = \frac{C_7}{q^2} 4m_b T_1(q^2) + C_9 \frac{V(q^2)}{M_B + M_{K^*}}, \quad (7.5)$$

$$C = C_{10} \frac{V(q^2)}{M_B + M_{K^*}}, \quad (7.6)$$

$$B_1 = \frac{C_7}{q^2} 4m_b T_2(q^2)(M_B^2 - M_{K^*}^2) + C_9 A_1(q^2)(M_B + M_{K^*}), \quad (7.7)$$

$$B_2 = - \left[\frac{C_7}{q^2} 4m_b \left(T_2(q^2) + q^2 \frac{T_3(q^2)}{(M_B^2 - M_{K^*}^2)} \right) + C_9 \frac{A_2(q^2)}{M_B + M_{K^*}} \right], \quad (7.8)$$

$$D_1 = C_{10} A_1(q^2)(M_B + M_{K^*}), \quad (7.9)$$

$$D_2 = -C_{10} \frac{A_2(q^2)}{M_B + M_{K^*}}. \quad (7.10)$$

The FB asymmetry is defined as

$$A^{\text{FB}}(q^2)$$

$$= \frac{\int_0^1 \frac{d^2\Gamma}{dq^2 d\cos\theta_{\ell}} d\cos\theta_{\ell} - \int_{-1}^0 \frac{d^2\Gamma}{dq^2 d\cos\theta_{\ell}} d\cos\theta_{\ell}}{\int_0^1 \frac{d^2\Gamma}{dq^2 d\cos\theta_{\ell}} d\cos\theta_{\ell} + \int_{-1}^0 \frac{d^2\Gamma}{dq^2 d\cos\theta_{\ell}} d\cos\theta_{\ell}}; \quad (7.11)$$

thus, we have

$$A^{\text{FB}}(q^2) = \frac{3}{4} \frac{2q^2(A_+^L + A_-^R - A_-^L - A_+^R)}{A_L + 2q^2(A_-^L + A_+^R + A_+^L + A_-^R)}. \quad (7.12)$$

$A^{\text{FB}}(q^2)$ is depicted in Fig. 6; it is consistent with the prediction of low asymmetry in the small q^2 region and high asymmetry for large q^2 . The analysis of the individual shapes of the helicity amplitudes (neglecting the long distance contribution) shows that A_+^L and A_+^R have comparable size, and therefore there is a cancellation of their contribution in Eq. (7.12); moreover, they are small with respect to A_-^L . In the region of large $M_{\ell^+\ell^-}^2$, A_-^L dominates over A_-^R , whereas the situation is reversed for low dilepton invariant mass squared, and this is the reason for the small positive asymmetry appearing in Fig. 6 for $M_{\ell^+\ell^-}^2 \leq 3 \text{ GeV}^2$. It is interesting to observe that such positive asymmetry depends on C_7 , and that it disappears if C_7 has a reversed sign.

The invariant-mass-squared distribution of the lepton pair is depicted in Fig. 7, where the short distance contribution is separately displayed. The predicted branching ratio is

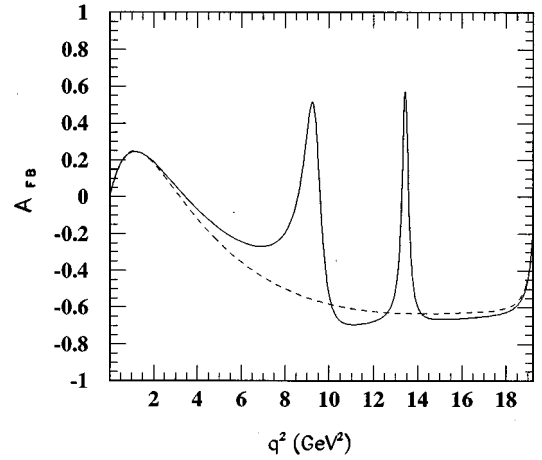


FIG. 6. Forward-backward asymmetry in the decay $B \rightarrow K^* \ell^+ \ell^-$; the dashed line refers to the short distance contribution only.

$B(B \rightarrow K^* \ell^+ \ell^-)|_{sd} = 1 \times 10^{-6} |V_{ts}/0.04|^2$, to be compared to the experimental upper limit $B(\bar{B}^0 \rightarrow K^{*0} \mu^+ \mu^-) < 3.1 \times 10^{-5}$ (CLEO II) and $B(\bar{B}^0 \rightarrow K^{*0} \mu^+ \mu^-) < 2.3 \times 10^{-5}$ (UA1) (at 90% C.L.) obtained excluding the region of the resonances J/ψ and ψ' [41,44,39]. Also in this case the uncertainty in C_9 does not have relevant consequences.

The interesting observation is that, for low values of the invariant mass squared, the distribution is still sizable, an effect that could be revealed at future B factories such as the Pep-II asymmetric e^+e^- collider at SLAC.

VIII. CONCLUSIONS

In this paper we have analyzed some features of the rare decays $B \rightarrow K \ell^+ \ell^-$ and $B \rightarrow K^* \ell^+ \ell^-$ within the theoretical framework provided by the standard model, using an approach based on three-point function QCD sum rules to compute the relevant hadronic matrix elements.

Albeit QCD sum rules have their own limitations (finite number of terms in the operator product expansion of the

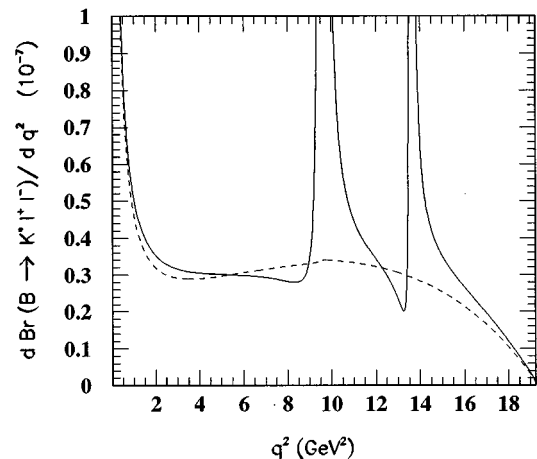


FIG. 7. Invariant-mass-squared distribution of the lepton pair for the decay $B \rightarrow K^* \ell^+ \ell^-$; the dashed line refers to the short distance contribution only.

correlators, values of the condensates, validity of the local duality assumption), we believe that the obtained results are meaningful from the quantitative point of view.

There is a quite good agreement with independent QCD methods (lattice QCD, light-cone sum rules) for a few quantities computed by the various approaches. The calculations of the remaining quantities (F_0 , T_i , A_0) by the other two methods is required in order to complete the overview on the various results.

We have used our results to test some relations among the computed form factors which hold in the infinite heavy quark limit, but that are expected to hold also for low values of q^2 and for finite b mass. We have found that the different form factors satisfy with different accuracies these relations, which can be explained by a different role of the $1/m_b$ corrections.

As for the decays we have analyzed in the present paper, within the standard model they are expected with branching ratios of the order 10^{-7} ($B \rightarrow K \ell^+ \ell^-$) and 10^{-6} ($B \rightarrow K^* \ell^+ \ell^-$), with peculiar shapes of the invariant mass of the lepton pair and of the FB asymmetry. Any deviation from the above expectations would be interpreted as a signal of deviation from the standard model. Interesting experimental data are therefore expected from current and future e^+e^- colliders in this exciting sector of the heavy flavor physics.

ACKNOWLEDGMENTS

We thank V.M. Braun, F. Buccella, G. Nardulli, and N. Paver for useful discussions.

APPENDIX A: $B \rightarrow K \ell^+ \ell^-$

The three-point function QCD sum rule for the form factor $F_T(q^2)$ in Eq. (3.2) can be derived by studying the function $\Pi(p^2, p'^2, q^2)$ in Eq. (3.4) and using in Eqs. (3.9), (3.11) the expressions

$$H = -2f_K f_B \frac{M_B^2}{m_b} \frac{1}{M_B + M_K}, \quad (A1)$$

$$\rho(s, s', q^2) = \frac{3}{2\lambda^{3/2}} \left\{ 2\Delta' s - \Delta u + \frac{1}{\lambda} [6\Delta'^2 s^2 + 2\Delta s s' - 6\Delta\Delta' s u + \Delta^2 u^2] \right\}, \quad (A2)$$

with $\Delta = s - m_b^2$, $\Delta' = s' - m_s^2$, $u = s + s' - q^2$, $\lambda = u^2 - 4s s'$. The coefficients of $D=3$ and $D=5$ vacuum matrix elements are given by

$$d_3 = 0, \quad (A3)$$

$$d_5 = \frac{m_b}{3r^2 r'^2}, \quad (A4)$$

with $r = p^2 - m_b^2$, $r' = p'^2 - m_s^2$.

Also $F_1(q^2)$ and $F_0(q^2)$ can be derived by equations analogous to (3.9), (3.11). The relevant quantities for $F_1(q^2)$ are given by

$$H = f_K f_B \frac{M_B^2}{m_b}, \quad (A5)$$

$$\begin{aligned} \rho(s, s', q^2) = & \frac{3}{8\lambda^{3/2}} \left\{ m_b [2\Delta(u - s') + \Delta'(u - 4s)] + m_s (\Delta u - 2\Delta' s) \right. \\ & \left. + \frac{2m_b}{\lambda} [\Delta^2(3s'u - 2ss' - u^2) + \Delta'^2(3su - 6s^2) + 2\Delta\Delta'(3su - 2ss' - u^2)] \right\}, \end{aligned} \quad (A6)$$

$$d_3 = -\frac{1}{2rr'}, \quad (A7)$$

$$d_5 = \frac{m_b^2}{4r^3 r'} + \frac{m_s^2}{4r r'^3} + \frac{1}{6r^2 r'} + \frac{2m_s^2 - m_s m_b - 2q^2}{12r^2 r'^2}. \quad (A8)$$

For $F_0(q^2)$ the formulas read

$$H = f_K f_B \frac{M_B^2}{m_b} (M_B^2 - M_K^2), \quad (A9)$$

$$\rho(s, s', q^2) = \frac{3}{8\sqrt{\lambda}} \left\{ \Delta(m_b - m_s) + \frac{2\Delta' s - \Delta u}{\lambda} \{m_b[2(\Delta - \Delta') + 2s' - u] + m_s(u - 2s)\} \right\}, \quad (\text{A10})$$

$$d_3 = -\frac{m_b(m_b - m_s)}{rr'}, \quad (\text{A11})$$

$$d_5 = (m_b - m_s) \left[\frac{m_b m_s^2}{2rr'^3} + \frac{m_b(m_b^2 - m_b m_s + m_s^2 - q^2)}{6r^2 r'^2} + \frac{m_b - m_s}{6rr'^3} + \frac{m_b^3}{2r^3 r'} + \frac{2m_b}{3r^2 r'} \right]. \quad (\text{A12})$$

In the formulas for the coefficients of the nonperturbative contributions, reported in this appendix and in the following one, we have omitted all terms that vanish after the double Borel transform.

APPENDIX B: $B \rightarrow K^* \ell^+ \ell^-$

The quantities appearing in the sum rule for the form factor $T_1(q^2)$ in Eq. (4.2) read

$$H = 2f_{K^*} M_{K^*} f_B \frac{M_B^2}{m_b}, \quad (\text{B1})$$

$$\begin{aligned} \rho(s, s', q^2) = \frac{3}{8\sqrt{\lambda}} \left\{ \Delta - \frac{1}{\lambda} \{m_b m_s [2\Delta' s + 2\Delta s' - u(\Delta + \Delta')] \right. \\ \left. + (s' - u)(2\Delta' s - \Delta u) - s(2\Delta s' - \Delta' u) - \Delta'^2 s - \Delta^2 s' + \Delta\Delta' u \} \right\}, \end{aligned} \quad (\text{B2})$$

$$d_3 = -\frac{(m_b + m_s)}{2rr'}, \quad (\text{B3})$$

$$d_5 = \frac{m_s}{12rr'^2} + \frac{3m_b + 2m_s}{12r^2 r'} + \frac{m_s^2(m_b + m_s)}{4rr'^3} + \frac{m_b^2(m_b + m_s)}{4r^3 r'} - \frac{(m_b + m_s)[m_b m_s + 2(q^2 - m_b^2 - m_s^2)]}{12r^2 r'^2}. \quad (\text{B4})$$

For the form factor $T_2(q^2)$,

$$H = -f_{K^*} M_{K^*} f_B \frac{M_B^2}{m_b} (M_B^2 - M_{K^*}^2), \quad (\text{B5})$$

$$\rho(s, s', q^2) = \frac{3}{16\sqrt{\lambda}} \left\{ m_b m_s (\Delta' - \Delta) + (\Delta s' - \Delta' s) + (u - 2s) \frac{(\Delta'^2 s + \Delta^2 s' - \Delta\Delta' u)}{\lambda} \right\}, \quad (\text{B6})$$

$$d_3 = \frac{(m_b - m_s)[(m_b + m_s)^2 - q^2]}{4rr'}, \quad (\text{B7})$$

$$\begin{aligned} d_5 = & -\frac{3m_b + m_s}{24rr'} - \frac{(m_b - m_s)m_s^2[(m_b + m_s)^2 - q^2]}{8rr'^3} - \frac{(m_b - m_s)m_b^2[(m_b + m_s)^2 - q^2]}{8r^3 r'} \\ & + \frac{(m_b - m_s)[(m_b + m_s)^2 - q^2][m_b m_s - 2(m_b^2 + m_s^2 - q^2)]}{24r^2 r'^2} + \frac{q^2(2m_b - m_s) - 2(m_b + m_s)(m_b^2 - m_s^2)}{24rr'^2} \\ & + \frac{q^2(5m_b - 4m_s) - 4(m_b + m_s)(m_b^2 - m_s^2)}{24r^2 r'}. \end{aligned} \quad (\text{B8})$$

For the form factor $V(q^2)$,

$$H = f_{K^*} M_{K^*} f_B \frac{M_B^2}{m_b} \frac{2}{M_B + M_{K^*}}, \quad (\text{B9})$$

$$\rho = -\frac{3}{4\lambda^{3/2}} [m_b(2\Delta s' - \Delta' u) + m_s(2\Delta' s - \Delta u)], \quad (\text{B10})$$

$$d_3 = -\frac{1}{rr'}, \quad (\text{B11})$$

$$d_5 = \frac{1}{3r^2r'} + \frac{m_b^2}{2r^3r'} + \frac{m_s^2}{2rr'^3} + \frac{2(m_b^2 + m_s^2 - q^2) - m_b m_s}{6r^2r'^2}. \quad (\text{B12})$$

For the form factor $A_1(q^2)$,

$$H = f_{K^*} M_{K^*} f_B \frac{M_B^2}{m_b} (M_B + M_{K^*}), \quad (\text{B13})$$

$$\rho = \frac{3}{8\sqrt{\lambda}} \left[(m_b \Delta' + m_s \Delta) + \frac{2m_b}{\lambda} (\Delta'^2 s + \Delta^2 s' - \Delta \Delta' u) \right], \quad (\text{B14})$$

$$d_3 = -\frac{1}{2rr'} [m_b^2 + m_s^2 - q^2 + 2m_b m_s], \quad (\text{B15})$$

$$d_5 = -\frac{1}{6rr'} + \frac{3m_b^2 + 9m_b m_s + 4m_s^2 - 4q^2}{12r^2r'} + \frac{4m_b^2 + 6m_b m_s + 6m_s^2 - 4q^2}{24r^2r'^2} + \frac{m_s^2[(m_b + m_s)^2 - q^2]}{4rr'^3} + \frac{m_b^2[(m_b + m_s)^2 - q^2]}{4r^3r'} \\ - \frac{-4m_b^4 - 6m_b^3 m_s - 4m_b^2 m_s^2 - 6m_b m_s^3 - 4m_s^4 - 4m_b^2 q^2 + 6m_b m_s q^2 + 8m_s^2 q^2 - 4q^4}{24r^2r'^2}. \quad (\text{B16})$$

For the form factor $A_2(q^2)$,

$$H = f_{K^*} M_{K^*} f_B \frac{M_B^2}{m_b} \frac{1}{M_B + M_{K^*}}, \quad (\text{B17})$$

$$\rho = -\frac{3}{8\lambda^{3/2}} \left\{ m_b(2\Delta s' - \Delta' u) + m_s(2\Delta' s - \Delta u) \right. \\ \left. + \frac{2m_b}{\lambda} [\Delta'^2(2ss' + u^2 - 3su) + 3\Delta^2(2s'^2 - s'u) + 2\Delta\Delta'(-3s'u + 2ss' + u^2)] \right\}, \quad (\text{B18})$$

$$d_3 = -\frac{1}{2rr'}, \quad (\text{B19})$$

$$d_5 = -\frac{1}{6r^2r'} + \frac{m_s^2}{4rr'^3} + \frac{m_b^2}{4r^3r'} + \frac{2m_b^2 + 2m_s^2 - 2q^2 - m_b m_s}{12r^2r'^2}. \quad (\text{B20})$$

- [1] S. Bertolini, F. Borzumati, and A. Masiero, in *B Decays*, edited by S. Stone (World Scientific, Singapore, 1992), p. 458.
- [2] CLEO Collaboration, M. S. Alam *et al.*, Phys. Rev. Lett. **74**, 2885 (1995).
- [3] CLEO Collaboration, R. Ammar *et al.*, Phys. Rev. Lett. **71**, 674 (1993).
- [4] For a review of the implications of the measurement of $b \rightarrow s \gamma$ see J. H. Hewett, in *Spin Structure in High Energy Processes*, Proceedings of the 21st SLAC Summer Institute on Particle Physics, Stanford, California, edited by L. De Porcel and C. Dunwoodie (SLAC Report No. 444, Stanford, 1994), p. 463.
- [5] A. Ali, T. Mannel, and T. Morozumi, Phys. Lett. B **273**, 505 (1991); A. Ali, G. Giudice, and T. Mannel, Z. Phys. C **67**, 417 (1995).
- [6] N. G. Deshpande, G. Eilam, A. Soni, and G. L. Kane, Phys. Rev. Lett. **57**, 1106 (1986); N. G. Deshpande and J. Trampetic, *ibid.* **60**, 2583 (1988).
- [7] W. Jaus and D. Wyler, Phys. Rev. D **41**, 3405 (1990); C. Greub, A. Ioannissian, and D. Wyler, Phys. Lett. B **346**, 149 (1995).
- [8] C. A. Dominguez, N. Paver, and Riazuddin, Z. Phys. C **48**, 55 (1990).
- [9] R. Casalbuoni, A. Deandrea, N. Di Bartolomeo, R. Gatto, and G. Nardulli, Phys. Lett. B **312**, 315 (1993).
- [10] M. A. Shifman, A. I. Vainshtein, and V. I. Zakharov, Nucl.

- Phys. **B147**, 385 (1979). For a review on the QCD sum rule method see the reprints volume *Vacuum Structure and QCD Sum Rules*, edited by M. A. Shifman (North-Holland, Amsterdam, 1992).
- [11] B. L. Ioffe and A. V. Smilga, Phys. Lett. **114B**, 353 (1982); Nucl. Phys. **B216**, 373 (1983); V. A. Nesterenko and A. V. Radyushkin, Phys. Lett. **115B**, 410 (1982); JETP Lett. **39**, 707 (1984).
- [12] M. Neubert, Phys. Rep. **245**, 259 (1994), and references therein.
- [13] P. Colangelo, G. Nardulli, A. A. Ovchinnikov, and N. Paver, Phys. Lett. B **293**, 207 (1992).
- [14] P. Colangelo, G. Nardulli, and N. Paver, Phys. Lett. B **269**, 204 (1991).
- [15] P. Ball, V. M. Braun, and H. G. Dosch, Phys. Rev. D **44**, 3567 (1991).
- [16] P. Ball, Phys. Rev. D **48**, 3190 (1993).
- [17] P. Colangelo, C. A. Dominguez, G. Nardulli, and N. Paver, Phys. Lett. B **317**, 183 (1993).
- [18] P. Ball, Report No. TUM-T31-43/93 (unpublished).
- [19] S. Narison, Phys. Lett. B **327**, 360 (1994).
- [20] B. Stech, Phys. Lett. B **354**, 447 (1995).
- [21] N. Isgur and M. B. Wise, Phys. Rev. D **42**, 2388 (1990).
- [22] G. Burdman and J. F. Donoghue, Phys. Lett. B **270**, 55 (1991).
- [23] B. Grinstein, M. J. Savage, and M. B. Wise, Nucl. Phys. **B319**, 271 (1989).
- [24] M. Misiak, Nucl. Phys. **B393**, 23 (1993); **B439**, 461(E) (1995).
- [25] A. Buras and M. Münz, Phys. Rev. D **52**, 186 (1995).
- [26] M. Ciuchini, E. Franco, G. Martinelli, L. Reina, and L. Silvestrini, Phys. Lett. B **316**, 127 (1993); M. Ciuchini, E. Franco, G. Martinelli, and L. Reina, Nucl. Phys. **B415**, 403 (1994); G. Cella, G. Curci, G. Ricciardi, and A. Viceré, *ibid.* **B421**, 41 (1994); Phys. Lett. B **325**, 227 (1994).
- [27] CDF Collaboration, F. Abe *et al.*, Phys. Rev. D **50**, 2966 (1994).
- [28] P. Colangelo, C. A. Dominguez, and N. Paver, Phys. Lett. B **352**, 134 (1995).
- [29] P. Colangelo and P. Santorelli, Phys. Lett. B **327**, 123 (1994).
- [30] V. M. Belyaev, A. Khodjamirian, and R. Rückl, Z. Phys. C **60**, 349 (1993).
- [31] UKQCD Collaboration, D. R. Burford *et al.*, Nucl. Phys. **B447**, 425 (1995).
- [32] P. Colangelo, F. De Fazio, and P. Santorelli, Phys. Rev. D **51**, 2237 (1995).
- [33] A. Ali, V. M. Braun, and H. Simma, Z. Phys. C **63**, 437 (1994).
- [34] UKQCD Collaboration, K. C. Bowler *et al.*, Phys. Rev. Lett. **72**, 1398 (1994); C. Bernard, P. Hsieh, and A. Soni, *ibid.* **72**, 1402 (1994).
- [35] UKQCD Collaboration, K. C. Bowler *et al.*, Phys. Rev. D **51**, 4955 (1995); APE Collaboration, A. Abada *et al.*, Report No. CERN-TH/95-59 (unpublished).
- [36] G. Burdman, Phys. Rev. D **52**, 6400 (1995).
- [37] C. S. Lim, T. Morozumi, and A. I. Sanda, Phys. Lett. B **218**, 343 (1989); N. G. Deshpande, J. Trampetic, and K. Panose, Phys. Rev. D **39**, 1461 (1989).
- [38] P. J. O' Donnell and H. K. K. Tung, Phys. Rev. D **43**, R2067 (1991); N. Paver and Riazuddin, *ibid.* **45**, 978 (1992).
- [39] For a recent review on the B meson phenomenology see T. E. Browder and K. Honscheid, Prog. Part. Nucl. Phys. **35**, 81 (1995).
- [40] For a determination of V_{ts} using heavy quark symmetries and data on the semileptonic $D \rightarrow K^* \ell \bar{\nu}$ decay see P. A. Griffin, M. Masip, and M. McGuigan, Phys. Rev. D **50**, 5751 (1994).
- [41] CLEO Collaboration, P. Avery *et al.*, Phys. Lett. B **183**, 429 (1987); **223**, 470 (1989); CLEO Collaboration, R. Balest *et al.*, Report No. CLEO CONF 94-4 (unpublished).
- [42] ARGUS Collaboration, H. Albrecht *et al.*, Phys. Lett. B **262**, 148 (1991).
- [43] D. Liu, Phys. Lett. B **346**, 355 (1995); Phys. Rev. D **52**, 5056 (1995).
- [44] UA1 Collaboration, C. Albajar *et al.*, Phys. Lett. B **262**, 163 (1991).